

EFFECT OF THE COLLECTOR GEOMETRY IN THE CONCENTRATING PHOTOVOLTAIC THERMAL SOLAR CELL PERFORMANCE

by

**Joao Paulo N. TORRES^{a*}, Joao F. P. FERNANDES^b, Carlos FERNANDES^a,
Paulo Jose COSTA BRANCO^b, Catarina BARATA^c, and Joao GOMES^d**

^a Telecommunications Institute, School of Engineering, University of Lisbon, Lisbon, Portugal

^b Institute of Mechanical Engineering, Associated Laboratory for Energy,
Transports and Aeronautics, School of Engineering, University of Lisbon, Lisbon, Portugal

^c Department of Electrical and Computer Engineering, School of Engineering,
University of Lisbon, Lisbon, Portugal

^d Solarus Sunpower AB, Gavle, Sweden

Original scientific paper

<https://doi.org/10.2298/TSCI171231273T>

*The aim of this work is the redesign of the reflector geometry in hybrid concentrating collectors that are currently manufactured by SOLARUS Sunpower AB** to improve the energy efficiency of their solar collectors. The analysis is first accomplished using a numerical model that uses geometrical optics to study the interaction between the sunlight and a concentrating collector along the year. More complex physical models based on open-source and advanced object-oriented Monte Carlo ray tracing programs (SolTrace, Tonatiuh) have been used to study the relation between the collector annual performance and its geometry. On an annual performance basis, a comparative analysis between several solar collector geometries was effectuated to search for higher efficiencies but with controlled costs. Results show that efficiency is deeply influenced by reflector geometry details, collector tilt and location (latitude, longitude) of the solar panel installation and, mostly, by customer demands. Undoubtedly, the methodology presented in this paper for the design of the solar collector represents an important tool to optimize the binomial cost/effectiveness photovoltaic performance in the energy conversion process. The results also indicate that some modified concentrating solar collectors are promising when evaluating the yearly averaged energy produced per unit area, leading to evident improvements in the performance when compared to the current standard solar concentrating SOLARUS systems. Increases of about 50% (from 0.123 kW/m² to 0.1832 kW/m²) were obtained for the yearly average collected power per reflector area when decreasing the collector height in 3.5% (from 143 mm to 138 mm).*

Key words: *hybrid solar collectors, panel efficiency, photovoltaic, renewable energy, shading, solar concentration*

Introduction

In a glossary of terms in sustainable energy regulation, Xavier Lemaire defines sustainable development as *which meets all the needs of the present without compromising the*

* Corresponding author; e-mail: joaotorres@tecnico.ulisboa.pt

** <http://www.bcorporation.net/community/solarus-sunpower-sweden-ab> and www.solarus.se

*ability of future generations to meet their own needs** [1]. Apart from the social aspects, the two other pillars of sustainability currently referred to are environmental and economic features. The former has enhanced the RES, the economic aspects deal with the energy efficiency. Among the most used alternatives within renewable energies, solar energy plays a fundamental role.

In the last few years, the costs of photovoltaic (PV) modules have dropped rapidly benefitting from technical improvements. Taking into account that the solar cells prices are still responsible for a great percentage of the overall costs related to conversion energy system, different techniques have been implemented to increase the solar energy production without the use of more solar cells. Example of this is the inclusion of reflector concentrators in the concentrating PV-thermal (C-PVT) collector to increase the solar irradiance in the solar cells [2, 3]. This may have a higher importance in world regions where the average irradiation is low. However, concentrators present some drawbacks, namely a decrease in the conversion efficiency, related to a partial absorption of the incident radiation by the reflector, and a reduction in the reflectivity features, related to dirt or aging [4, 5]. Additionally, the temperature of PV panels can exceed 100 °C on certain roofs during summer: thousands of PV parks experience a loss of productivity due to the panel heating, which leads to a decrease in the conversion efficiencies and a fail to reach their nominal capacity. Therefore, in the PV conversion system, cooling is crucial [6].

The PV and thermal collectors, also known as hybrid, offer the possibility of obtaining both thermal and electrical energy from the same collector and, simultaneously, avoiding the increase in the solar cell temperature, due to heat removal in the thermal system [7]. The achieved cooling effect in the electric part of PV and thermal (PVT) collectors is referred to increase by roughly 20% the annual electric output, when compared to conventional solar PV panels [8]. The SOLARUS AB uses (C-PVT) technology [9], in order to improve the energy efficiency of the overall system.

The paper focuses:

- (1) the redesign of the reflector geometry of the C-PVT collector manufactured using the SOLARUS Sunpower AB technology, and
- (2) the description of an adequate methodology for future optimizations.

Regarding the first point, the reflector geometry was altered to visualize its impact on the monthly power collected in the concentrator side of the C-PVT, considering several tilt angles and for different periods of the year. For instance, it was analyzed the impact on the absorbed energy when small differences in the concentrator profile were taken into account. These particular solutions led to different energy absorptions for different tilt angles, which can always be adjusted to the consumption profile or to the local sun altitude. The influences of heat pipe cross-section geometry and water dynamics in the heat removal of the PVT collector were not considered.

With the increasing use of optimizations tools, such as the generic algorithms (GA), it is crucial to adapt or create fast and accurate calculation tools. Regarding the second point, most commercial tools are able to calculate very precise solutions, but often present constraints related to the computation time and to its interface to other tools.

In this article, the performance of different collector structures is evaluated using advanced ray tracing programs (Tonatiuh, SolTrace...). On an annual performance basis, different collector geometries were assessed searching for higher efficiency but with con-

* <http://theconversation.com/profiles/xavier-lemaire-156025>

trolled costs. More complex procedures, beyond the scope of the present work, use subsequently the results from the simulations to guide the GAs search towards finding low cost/high efficiency solutions to the specific problem under study.

This self-consistent calculation is usually associated with high computing times. Even with fast numerical simulation models (for instance, tens of seconds per structure), the use of 100 elements and 100 generations can lead to optimization processes that can last up to several days or weeks [10]. In a simplified 2-D model, sufficiently precise solutions can be guaranteed with a drastically reduced running time. Despite a reduction in accuracy, this will in fact represent an important trade-off in optimization processes.

Detailed description of a simple simulation model for 2-D calculations based on MATLAB software and geometrical optics to study the influence of the collector geometry on the annual performance of the solar panel, is presented. Also, results considering the influence of several collector parameters in the solar panel performance, namely the geometry of the collector (reflector shape, reflector height, aperture, location of the receiver inside the collector) in a 2-D analysis, has been shown. However, other parameters are determinant in the main features of the solar panels, such as: the orientation (tilt), latitude, azimuth, annual irradiance distribution and commercial applications. A more complete physical model making use of an open-source advanced object-oriented Monte Carlo ray tracing program, such as SolTrace [11] or Tonatiuh [12, 13], is required for 3-D calculations, to obtain the light distribution along the receiver. The respective results are also shown and discussed along with a comparative analysis between the proposed collectors and the current solar modules of Solarus AB.

The solar collector

The solar collector produced by SOLARUS AB and shown in fig. 1(a) is used as the reference one in the comparative analysis made all along this paper. It is a C-PVT asymmetrical collector, generally referred as compound parabolic collector (CPC), and belongs to the maximum reflector concentrator (MaReCo) family [14]. The collector has two identical troughs, which are both composed by a receiver (and respective absorber), two rows of monocrystalline PV cells (one on the top and the other on the bottom of the receiver), a reflector, a frame of plastic and metal (aluminium) to support the entire system and an antireflective protection cover in transparent glass (glazed protection cover), in which the solar transmittance is 95%.

The set of C-PVT upper cells behave as a normal flat receiver, however, the bottom cells only collect the solar radiation forwarded by a reflector. In currently manufactured SOLARUS modules, the strings have 19 or 38 solar cells series connected, as seen in fig. 1. To mitigate the effects of partial shading or to the non-uniformity of the light distribution in the receiver, bypass diodes are included. In standard SOLARUS MaReCo configurations, the strings of cells in the receiver are formed by 4 groups of solar cells, each one with its bypass (BP) diode.

The standard cell is $0.156 \text{ m} \times 0.156 \text{ m}$. To fit within the collector design, the cell is cut to $0.148 \text{ m} \times 0.156 \text{ m}$. When the larger dimension is cut into three slices, it results a solar cell known as 1/3 cell, whose area A_{cell} is $0.148 \text{ m} \times 0.052 \text{ m}$, if it is divided into six slices, a solar 1/6 is formed ($A_{\text{cell}} = 0.148 \text{ m} \times 0.026 \text{ m}$), fig. 1(b).

Figure 1(a) shows the aperture area A_{aper} of the concentrating side of the collector, which corresponds to the opening area through which the Sun rays enter to the concentrating side of the receiver. The absorber contains a fluid, which can be antifreeze, water or both. This fluid flows through eight elliptic tubes and it is used for cooling of the PV cells [15, 16].

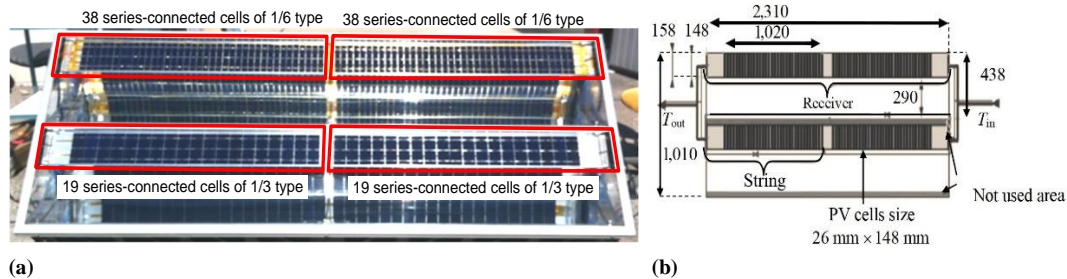


Figure 1. The PVT CPC standard modules produced by SOLARUS AB with the identification of its components; (a) collector top view and (b) electric part (all dimensions in mm)

In tab. 1 the main specification of the panel can be seen.

Table 1. Panel specifications

Weight	55 kg
Aperture area	2.2 m ²
Gross area	2.4 m ²
Cover	4 mm anti reflective glass, super transparent, hailstone safe
Frame	Anodized aluminum and ABS ASA plastic
Electric	
Number of cells	152
Cell dimension	55 mm × 148 mm × 240 mm
Maximum power rating at STC	250 Wp ±5%
Maximum power current	3.7 A
Maximum power voltage	40 V
Short circuit current	4.1 A
Open circuit voltage	51 V
Thermal	
Thermal isolation	4.8 W/m ² K
Absorber material	Aluminum
Peak power	1250 W/power collector
Capacity antifreeze	1.4 L/power collector
Maximum working pressure	10 bar
Operating pressure	6 bar
Stagnation temperature	180 °C
Permissible location	Roof, façade, ground, <i>etc.</i>
Installation method	Stationary or tracking

The 2-D numerical model

A very simple and flexible numerical model has been developed based on the principles of geometrical optics, which means that the propagation of solar radiation is made in terms of rays. The reflector acts like a mirror, receiving those rays and reflecting them. The analysis of those reflections is made obeying to the reflection law, given by:

$$\theta_i = \theta_r \quad (1)$$

In eq. (1) and illustrated in fig. 2(a), θ_i is the angle between the incident solar ray and the normal to the reflector plane and θ_r is the angle between the reflected solar ray and the normal to the reflector plane. The present version of the numerical model does not consider either energy losses in each reflection or even reflections of the solar radiation in the glass that covers the collector.

Several collector geometries were tested. However, none analysis along the trough axis was included. In fact, in most cases, the radiation distribution is almost uniform along this direction [9], which does not happen orthogonally to the trough axis. Therefore, the analysis of the radiation distribution in the transversal plane to the trough axis is relevant for the knowledge of either the collected energy or the achieved lighting uniformity level along the bottom side of the receiver.

Although it is being a 2-D numerical model, its results may accurately describe the temperature distribution in the vicinity of the strings

of solar cells and thus they may be used as input data for the thermal analysis of the C-PVT collector [17]. For each irradiance, G , and ambient temperature, T , conditions, the number of rays, N_R , that reaches the bottom of the receiver is enumerated. The average power in the receiver is thus proportional to this number and to the power per ray in the receiver, P_{ray} .

Several simulations were made using the numerical model for each irradiance-ambient temperature pair (G , T) to optimize the reflector geometry and its dimensions. Due to the computational complexity involved, a compromise between accuracy and computation time was taken into account, either varying the number of reflector sections (2, 4, 8, 16, and 32 sections), as illustrated in fig. 2(b), or/and the number of solar rays that enter in the concentrating side of the collector (10, 50, 100, 500, 1000, 5000, and 10000). Results have shown that 16 sections in the reflector discretization and 1000 incident rays are representative enough to insure an average error less than 1%

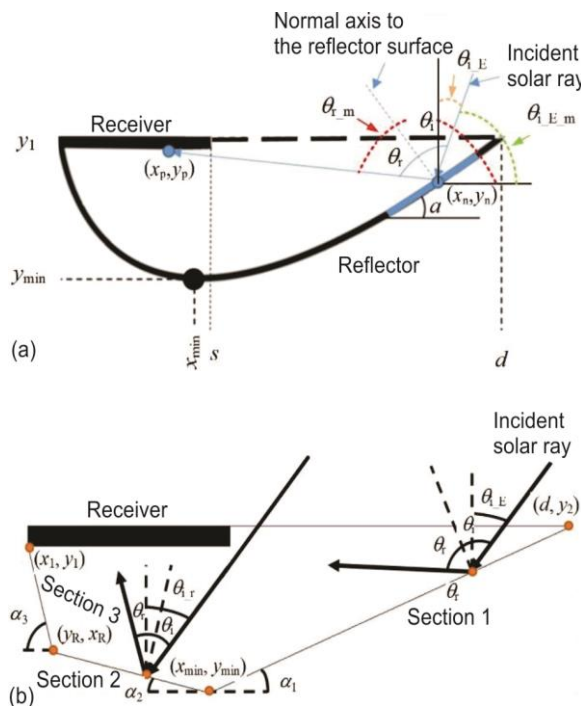


Figure 2. Simplified scheme of the C-PVT SOLARUS collector (a) and reflector discretization in straight sections (b)

when compared with the 32 sections/10000 rays case. Solar irradiance and incidence ray angles were obtained by numerical computation with real data for Gavle, Sweden [18, 19]. Its geographic co-ordinates (60.675° N, 17.142° E) were obtained through Google Maps and weather conditions, such as the wind and rain, were taken into account. Figure 2(b) shows the flowchart of the algorithm that was implemented in the simulations for each month of the year.

In the analysis using the 2-D numerical model, the following assumptions were considered:

- uniformed distribution along the collector axis,
- negligence of the shading effects associated with the presence of a collector frame, and
- the Sun path is described by a 2-D function (variable elevation solar angle α_s and a fixed azimuthal angle γ).

Computation of the reflection angles

In the flowchart presented in fig. 3, the computation of solar reflections is made. Those calculations were based on the reflection law at each point of the reflector. Each section that composes the reflector is defined by a slope α . For left side sections of the reflector (negative slope), the incident angle is given:

$$\theta_i = \theta_{i_E} + \alpha \quad (2)$$

In eq. (2), θ_{i_E} is the angle between the incident solar ray and the normal to the ground surface, as shown in fig. 3. For computation purposes, it is convenient to define a new reference (MATLAB reference). Accordingly, new incident and reflected angles are obtained, being given:

$$\theta_{i_{E_m}} = 90^\circ - \theta_{i_E} \quad (3)$$

$$\theta_{r_m} = 2\theta_i + \theta_{i_{E_m}} \quad (4)$$

For sections of the right side of the reflector (positive slope), eq. (4) is still valid and eq. (2) is replaced:

$$\theta_i = (\alpha + 90^\circ) - \theta_{i_{E_m}} \quad (5)$$

For multiple reflections, new values are obtained for θ_i and θ_{r_m} in a different section of the reflector, taking into account its slope α .

For left side sections:

$$\theta_i = (\alpha - 90^\circ) - (\theta_{r_{m_a}} - 180^\circ) \quad (6)$$

$$\theta_{r_m} = 2\theta_i + (\theta_{r_{m_a}} - 180^\circ) \quad (7)$$

$$\theta_i = (\alpha + 90^\circ) - (\theta_{r_{m_a}} - 180^\circ) \quad (8)$$

In eqs. (6) and (7), $\theta_{r_{m_a}}$ is the angle related to the reflection from the previous section. For right side sections, eq. (7) is still valid, but eq. (6) should be replaced by:

$$\theta_i = (\alpha + 90^\circ) - (\theta_{r_{m_a}} - 180^\circ) \quad (9)$$

For clarity purposes, incident and reflected rays are represented in fig. 2(b), for single reflections, and in fig. 4, for multiple reflections.

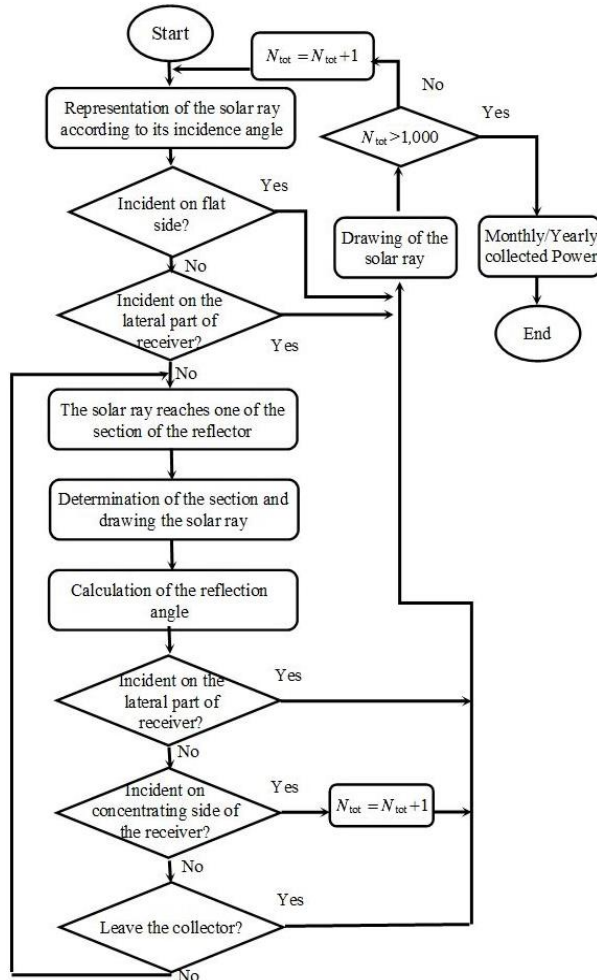


Figure 3. Flowchart with the model procedure

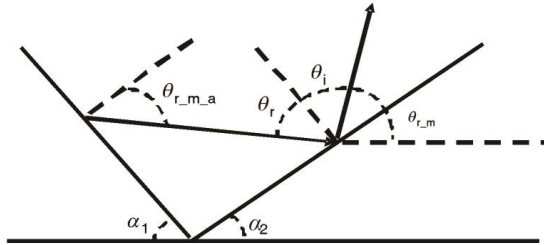


Figure 4. Ray path (reflection) between a section with negative slope and a section with positive slope

Computation of the average power in the bottom side of the receiver

In the flowchart presented in fig. 3, the computation of the average power is also made. The power related to the incident radiation in the reflector, P_{ref} , as shown in fig. 2(a), is associated to the aperture area A_{aper} and to the irradiance value G , being given by:

$$P_{ref} = A_{aper} G \quad (10)$$

The average power in the concentrating side of the receiver, P_{rec} , is related to the rays that enter through the aperture area of the glass cover, represented by N_{tot} . The number of rays, N_R , that reaches the bottom side of the receiver, which is a percentage of N_{tot} , is then registered. Notice, however, that these rays are no uniformly distributed along the receiver area, due to the concentration features of the reflector. The average power in the receiver P_{rec} is given by:

$$P_{rec} = P_{ref} \left(\frac{N_R}{N_{tot}} \right) = (A_{aper} G) \left(\frac{N_R}{N_{tot}} \right) \quad (11)$$

In eq. (11), P_{ref} is a fraction of the solar power that reaches the Earth's surface and that efficiently enters in the concentrating side of the collector. In the simulation procedure, the solar radiation entering through the aperture area was discretized into groups containing 1000 rays. The number N_R of solar rays that reaches the bottom side of the receiver is an indicator of the power that in a given moment of the day effectively reaches the receiver.

Numerical results

The 2-D simulation model was applied to the analysis of concentrating collector panels with different geometries. The algorithm allows the evaluation of the instantaneous power in the receiver, the areas of the reflectors and the light distribution along the bottom part of the receiver. For comparative reasons, SOLARUS panel shown in fig. 1 was considered as the reference or standard collector geometry. As fig. 2(a) shows, this panel has an asymmetrical CPC reflector and an asymmetrically placed receiver inside the collector.

The geometry of this collector is defined by the following set of parameters, as indicated in fig. 5: $L_{aper} = 287$ mm, $L_r = 143$ mm, $h = 143$ mm. The total length of the collector along the trough is $L_{tr} = 2310$ mm. Both parabolas that constitute the reflector has the same optical axis, which is orthogonal to the glass cover (90° of acceptance angle θ_a when the glass cover tilt θ_t is 0°). In the present analysis, the following collector geometries were performed:

- the SOLARUS C-PVT standard panels for θ_t equal to 0° , 15° , 30° , and 45° , in comparative studies with the results presented in [9], aiming at the validation of the proposed numerical model,
- the SOLARUS C-PVT reflectors in which the minimum of the reflector curve was lowered/raised on the optical axis for $\theta_t = 0^\circ$, 15° , and 30° ,
- the SOLARUS C-PVT reflectors in which the minimum of the reflector curve was moved in the plane orthogonal to the optical axis, for $\theta_t = 0^\circ$, 15° , and 30° , and
- the PVT symmetrical parabolic collectors with different locations of the receiver inside the collector.

Figure 5 represents schematically the standard SOLARUS C-PVT collector with an acceptable angle $\theta_a = 90^\circ$ and a cover glass tilt θ_t .

Other parameters related to the location and installation details of the solar panel are equally important for its complete description: the latitude (N or S), the longitude (W or E), the elevation solar angle α_s and the azimuthal angle γ , fig. 6. The angle α_s is obtained from [20], while the incident radiation angle ν is given:

$$\nu = 90 - (\alpha_s + \theta_t) \quad (12)$$

The influences of the height of the reflector h and tilt θ_t on the energy production of the overall collector have also been considered. The obtained results related to a 2-D simulation analysis have been compared with experimental ones provided by SOLARUS and also compared with simulation results obtained by others to validate the numerical model being used.

Solar collectors that concentrate the solar radiation are conceived to operate at a given tilt angle θ_t [21]. For the dimensions assumed for the standard MaReCo under analysis, the tilt angle is around 35° , but this can change according to the collector dimensions. The equation of the reflector curve was obtained through a set of data points provided by SOLARUS.

A good approach for the reflector geometry shows that its profile can be divided in three sections: an upper parabola, a circle, and a lower parabola.

In the 2-D calculation of the collected energy per month, real values for the solar irradiance were used, *i. e.*, values in which meteorological aspects were not discarded, such as wind and rain.

Simulations were performed for the SOLARUS AB standard reflector with collector tilts θ_t equal to 0° , 15° , 30° , and 45° . Results concerning the collected energy in the bottom part of the receiver along the year are plotted in fig. 7.

It is apparent in fig. 7 that the average power in the bottom part of the receiver P_{conc} increases with θ_t when the collector's surface area gets more exposed to the solar radiation. However, this increase in P_{conc} only happens until a certain tilt (here, for example, a tilt of 45°). The collector presents $\theta_a = 90^\circ$ when $\theta_t = 0^\circ$, but the acceptance angle decreases proportionally to the increase of the collector tilt. An excessive tilt θ_t will lead to a significant reduction (cut-off) in the collected energy during the summer months, as shown in fig. 7 for 45° , when the solar altitude reaches the year greatest values. Notice that this effect may be benefit if the client demands are searching for a more uniform yearly energy production.

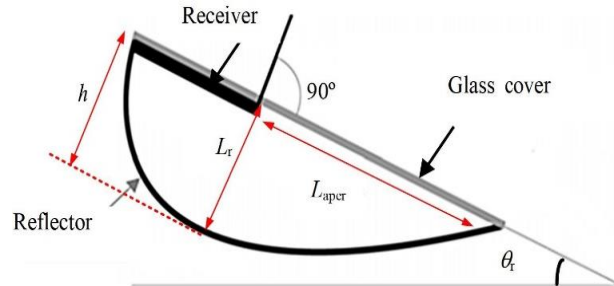


Figure 5. Schematic representation of the standard SOLARUS C-PVT collector with $\theta_a = 90^\circ$

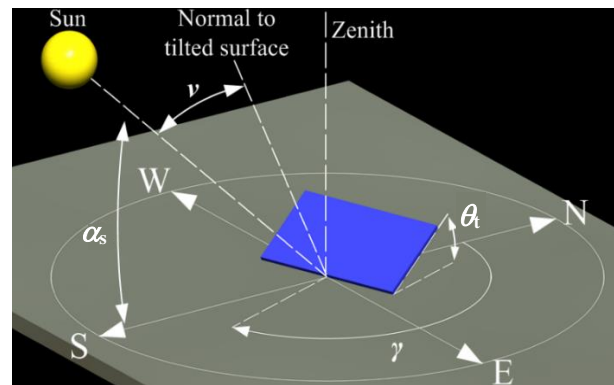


Figure 6. Schematic representation of the azimuthal, altitude and tilt angles for a given solar cell panel

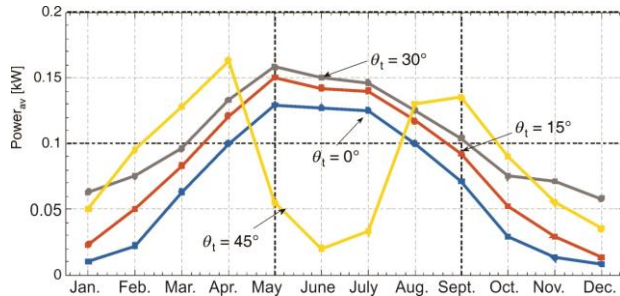


Figure 7. Average power in the bottom part of the receiver in the SOLARUS AB standard collector for θ_i of 0° , 15° , 30° , and 45° (results obtained with the 2D model)

In order to validate the numerical model, each curve presented in fig. 7 is compared with the ones shown in fig. 8, which were obtained in similar conditions by a 3-D analysis that uses a Monte Carlo ray tracing software known as Tonatiuh*. This software is very robust and flexible, once the instantaneous collected power values were acquired for each hour of the year, resulting in 8760 simulations per year. However, the weather aspects were neglected.

In fig. 8, it is noticed a *cut-off* on the collected power in the concentrating part of the collector for a 45° tilt. That is also visible in fig. 7 and occurs near the summer solstice (summer months) due to a significant decrease in the acceptance angle of the collector in its concentrating side. This phenomenon was already noticeable for a collector tilt of 30° , precisely in June, in which the solar altitude is the highest of the whole year.

The differences found in the figs. 7 and 8 are due to the light distribution along the receiver and due to the 3-D Sun path, which was not considered in the 2-D model. These differences are more concentrated in the months of winter, when the Sun has a wider path with a lower solar latitude. The average deviations (RMSE) between results, for the months of summer and winter, were 8.4% and 16.1%, respectively.

As main remarks of the presented examples, one can assume that the adopted numerical model is adequate and that the MaReCo collector under consideration is conceived to operate at a tilt around 35° .

Next step in our research was to apply the numerical model to include alterations in the collector geometry. Several types of modifications have been considered in the standard

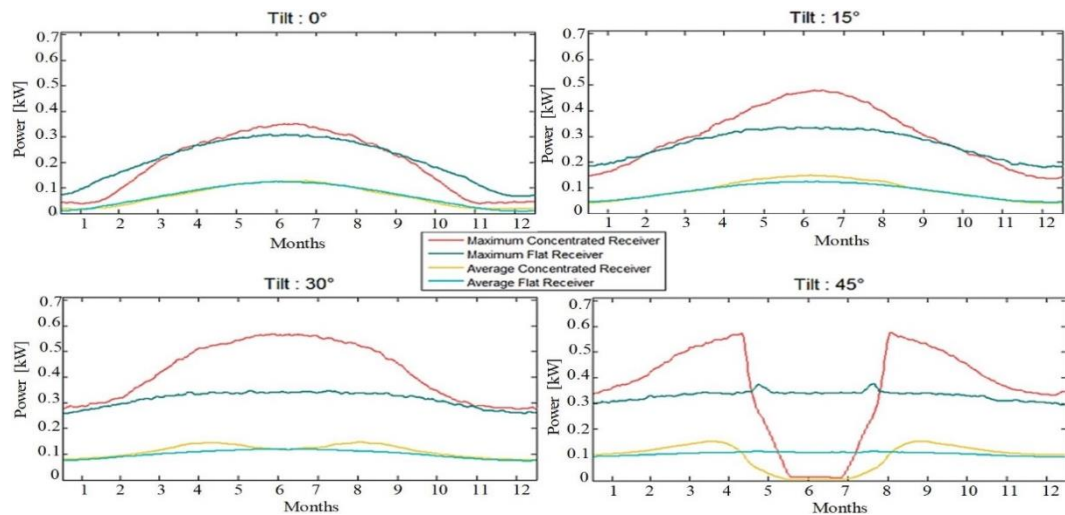


Figure 8. Daily maximum and average power values related to each receiver side (Tonatiuh)

* Tonatiuh is a Monte Carlo ray tracing software, which allows the optic simulation of solar concentrating systems

MaReCo collectors, basically corresponding to the displacement of the minimum point of the reflector MaReCo profile in the orthogonal plane of the collector axis. All of the proposed reflector configurations are parabolic type: some are asymmetric while others are symmetric.

The results in terms of collected power/area for the best configurations are shown in fig. 9. Reflector 1 corresponds to an asymmetric reflector with the $h = h_{\text{stand}} - 5$ mm. Reflector 2 corresponds to the reflector's minimum aligned with the extreme point of the receiver. At last, reflector 3 corresponds to the symmetric parabolic case, fig. 10.

These solutions are summarized in tab. 2. Concerning the collected power, the proposed MaReCo structures did not improve the standard SOLARUS panel in terms of produced energy. However, the power density per active area may be significantly increased in some new configurations. This figure of merit may be considered an added value, since it defines new structures that are economically more profitable than the actual standard SOLARUS AB reflector.

It is relevant to notice in fig. 9 that reflectors 1 and 2 have higher average power per area than the standard SOLARUS AB reflector, but they produce less energy per year. On the other hand, standard SOLARUS reflector and reflector 3 are very similar in terms of energy production.

Table 2. General data obtained for the best reflectors

	SOLARUS AB	Reflector 1	Reflector 2	Reflector 3
Yearly average of collected power [kW]	0.232	0.227	0.226	0.229
Reflector area [m ²]	1.881	1.240	1.238	1.870
Averaged collected power/reflector area [kWm ⁻²]	0.123	0.1835	0.1832	0.123

Next, using a 3-D simulation, the SOLARUS AB and the symmetric reflector 3 are compared. It is important to check the behaviour of the reflectors during the months of summer and winter and for different tilt angles θ .

Results of the 3-D simulation using SolTrace software

The symmetric parabolic reflector (reflector 3 in tab. 2) and the SOLARUS AB reflector present similar values either for the reflector areas or for the ratios (averaged collected power/reflector area). In order to understand why these two geometries present almost the same yearly performance, a more detailed analysis was implemented using a 3-D software.

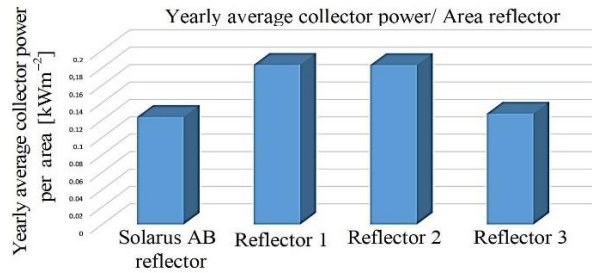


Figure 9. Yearly average of the collected power/area for the three best proposed reflector geometries and for the SOLARUS AB standard reflector

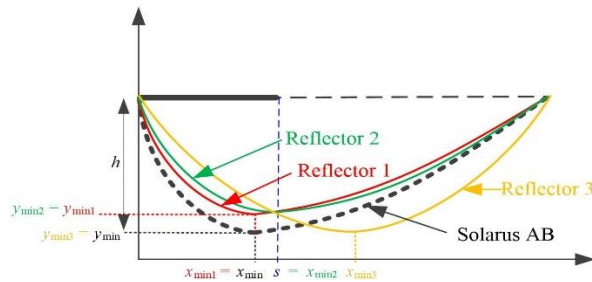


Figure 10. Geometry of reflectors 1 to 3 compared with the SOLARUS AB reflector

The results presented in this section were obtained using the software SolTrace. A comparative analysis was made between a standard MaReCo collector and a simple parabolic collector with the same dimensions h , L_r , and L_{aper} . The schematic design of each structure is presented in fig. 11.

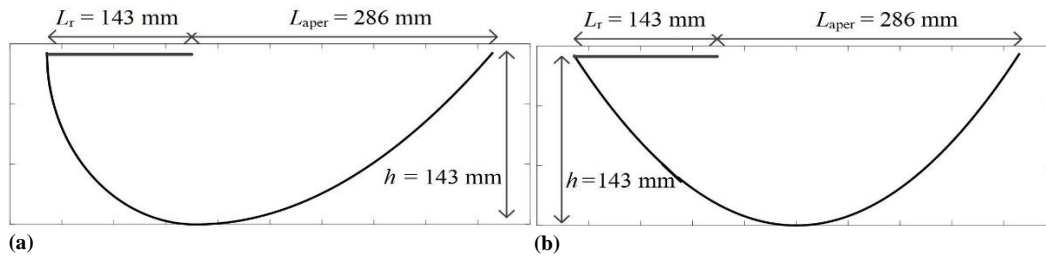


Figure 11. Schematic design of the PVT structures under 3-D analysis; (a) SOLARUS AB reflector and (b) symmetric parabolic reflector

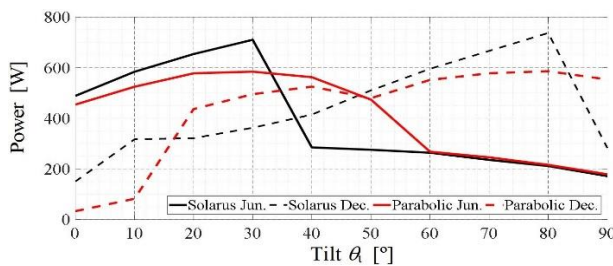


Figure 12. Collector absorbed power in function of tilt of the SOLARUS and the symmetric parabolic reflectors, at midday on the 21st of June and December

Figure 12 shows the influence of tilt angle θ on the instantaneous power collected when α_s (solar altitude) is maximum. In the figure, results are plotted for the SOLARUS MaReCo and for the parabolic reflector. All results were done for the location of Gavle, Sweden, at 12:00 hours local time on the 21st June and 21st December.

During June, the SOLARUS and the parabolic symmetric reflectors have its optimum points at $\theta = 30^\circ$. However, for December its maximum occurs for $\theta = 80^\circ$ (SOLARUS) and for $\theta = 40^\circ$ (parabolic reflector). According to fig. 11, if both SOLARUS and symmetric parabolic reflectors were installed with $\theta = 30^\circ$, it is expected for the SOLARUS reflector to produce more energy during the months of summer, while the symmetric parabolic would be a more adequate option during the months of winter. To verify this, it was computed the collector absorbed power for both cases, for each hour on the 21st of June and December. The results are plotted in fig. 13.

It is worth noticing the results concerning the power curve during the whole day in more detail. While in June the SOLARUS design absorb more energy during the period of the highest solar altitude α_s (from 10:00 to 14:00 hours), for the remaining part of the day the symmetric parabolic collector is more efficient. In December, the roles are reversed (from 10:00 to 14:00 hours the symmetric solution is better, in the sunset and sunrise, the standard collector is more efficient).

Summarizing, for those cases where the demand is higher at midday, SOLARUS collector should be chosen, on the contrary, if a consumer needs more energy outside the hours of the highest solar altitudes (for example a domestic consumer), then the symmetric parabolic design will be the right choice.

Another important aspect to be analysed is the monthly energy produced during the whole year, for both cases. The results can be seen in fig. 14. As shown in tab. 2, the total ene-

ergy produced by both designs are similar (correspond to the area below each curve in fig. 13, 1364 kWh and 1340 kWh for the SOLARUS and the parabolic cases, respectively). In fig. 14 it can be seen that the SOLARUS AB collector will absorb more energy during the months of summer and the symmetric parabolic collector is more efficient in winter.

In different words, SOLARUS AB design collects more energy for highest solar altitudes. The symmetric parabolic design collects more energy for lower solar altitudes, but again the energy collected in both cases are similar.

Results shown in figs. 12-14 reveal to be indispensable to choose the more convenient collector geometry for the consumer's design. With the combination of the hourly and annual demand profile of the consumers, these curves will help the decision makers to choose the more adequate design.

Conclusions

Simulation represents a powerful tool to investigate the influence of the collector geometry on the performance of the solar panel on an effectiveness/cost basis. The advantages of the simulation studies lie mainly in its flexibility, that is in the possibility of changing several parameters in the reflectors without much effort, and to ensure faster and cheaper analysis.

The 2-D and 3-D simulation analysis of several PVT collectors have been presented using ray tracing models. Annual distribution of the solar radiation over the bottom part of the receiver for several reflector geometries have been obtained for the case of PVT solar panels installed in Gavle, Sweden. Some of the proposed collector geometries have shown important improvements when compared to the flat and standard MaReCo structures manufactured by SOLARUS AB. Several aspects related to the daily and yearly distributions of the collected power were highlighted for a better fitting of the consumer's needs. The energy absorbed for different hours of the day and for different seasons of the year were considered in order to perform an adequate match between the collector energy production and the consumer's demand curves.

Small modifications in the geometry of the SOLARUS MaReCo collector led to increases of about 50% in the yearly average collected power per reflector area. Even for similar yearly average collected power per reflector area values, it is possible to obtain different energy collected distributions along the year. Results have shown that the SOLARUS

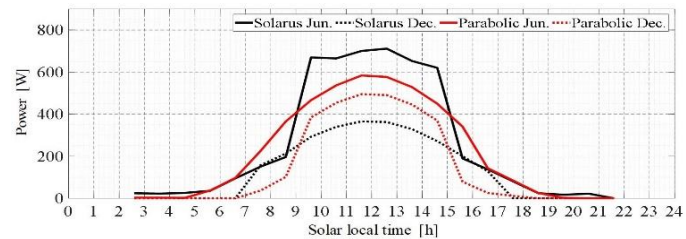


Figure 13. Collected power for different hours in the month of June and December for SOLARUS AB and for the symmetric parabolic designs (tilt 30°)

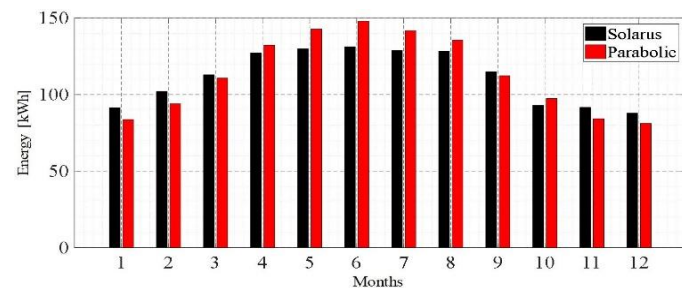


Figure 14. Monthly energy collected for SOLARUS AB and for the symmetric parabolic designs

MaReCo collector absorbs more energy during the months of summer and the symmetric parabolic collector in the months of winter.

The obtained results seem to be encouraging for the use of symmetrical geometries (both in the reflector and the receiver designs) to explore new markets located in lower latitudes, where there is a smoother distribution of the energy collected along the year.

This work is a previous study aiming at the use of the GA as a generative and search procedure of optimized solutions for the solar collector geometries related to hybrid concentrator panels in terms of the thermal/electric energy production performances and costs.

Acknowledgment

This work was supported by national funds through the Fundação para a Ciência e a Tecnologia (FCT) of the Portuguese Government with reference UID/EEA/50008/2013, and also supported by FCT, through IDMEC, under LAETA, project UID/EMS/50022/2013.

Nomenclature

A_{aper} – aperture area of the collector, [m²]
 A_{cell} – solar cell active area, [m²]
 G – solar irradiance, [Wm⁻²]
 h – collector height, [m]
 h_{stand} – collector height for the standard MaReCo collector, [m]
 L_{aper} – aperture length, [m]
 L_{r} – receiver length, [m]
 L_{tr} – collector length along the trough axis, [m]
 N_{R} – number of rays that reaches the bottom of the receiver, [-]
 N_{tot} – number of rays that enter through the aperture area, [-]
 P_{conc} – power in the concentrated (bottom) side of the receiver, [W]
 P_{ray} – power per ray in the receiver, [W]
 P_{rec} – average power in the receiver, [W]
 P_{ref} – average power in the reflector, [W]
 T – absolute temperature, [K]

ν – incident angle, [°]
 θ_{a} – acceptance angle, [°]
 θ_{i} – angle between incident solar ray and the normal to the reflector plane, [°]
 θ_{im} – angle between incident solar ray and the normal to the ground surface, [°]
 θ_{Em} – θ_{E} in MATLAB reference, [°]
 θ_{r} – angle between reflected solar ray and the normal to the reflector plane, [°]
 θ_{rE} – angle between reflected solar ray and normal to the ground surface, [°]
 θ_{rEm} – θ_{rE} in MATLAB reference, [°]
 θ_{t} – tilt angle of the glass cover, [°]

Acronyms

C-PVT – concentrating PV and thermal
 CPC – compound parabolic concentrator
 GA – genetic algorithms
 MaReCo – maximum reflector concentrator
 PV – PV
 PVT – PV and thermal

Greek symbols

α – slope of the reflector section, [°]
 α_{s} – elevation solar angle, [°]

References

- [1] Lemaire, X., Glossary of Terms in Sustainable Energy Regulation, REEEP/Sustainable Energy Regulation Network, Glossary, Warwick Business School, Coventry, UK, 2004
- [2] Muthu Manokara, A., *et al.*, Performance Analysis of Parabolic trough Concentrating PV Thermal System, *Procedia Technology*, 24 (2016), July, pp. 485-491
- [3] Xuan Tien, N., Shin, S., A Novel Concentrator PV (CPV) System with the Improvement of Irradiance Uniformity and the Capturing of Diffuse Solar Radiation, *MDPI Applied Sciences*, 6 (2016), 9, pp. 1-15
- [4] Fernandes, C. F., *et al.*, Aging of Solar PV Plants and Mitigation of their Consequences, *Proceedings, 17th International Conference on Power Electronics and Motion Control IEEE-PEMC*, Varna, Bulgaria, 2016
- [5] Ndiaye, A., *et al.*, Degradation Evaluation of Crystalline-Silicon PV Modules after a Few Operation Years in a Tropical Environment, *Solar Energy*, 103 (2014), May, pp. 70-77
- [6] Dubey, S., *et al.*, Temperature Dependent PV (PV) Efficiency and its Effect on PV Production in the World – A Review, *Energy Procedia*, 33 (2013), June, pp. 311-321

- [7] Zhou, Y., *et al.*, Performance of Buildings Integrated with a PV-Thermal Collector and Phase Change Materials, *Procedia Engineering*, 205 (2017), Nov., pp. 1337-1343
- [8] Castanheira, A. F. A., *et al.*, Demonstration Project of a Cooling System for Existing PV Power Plants in Portugal, *Applied Energy*, 211 (2018), Feb., pp. 1297-1307
- [9] Giovinazzo, C. L., *et al.*, Ray Tracing Model of an Asymmetric Concentrating PVT, *Proceedings*, Eurosun 2014, Aix-les-Bains, France, 2014, pp. 16-19
- [10] Youssef, A. M. A., *et al.*, Genetic Algorithm-Based Optimization for PVs Integrated Building Envelope, *Energy and Buildings*, 127 (2016), Sept., pp. 627-636
- [11] ***, National Renewable Energy Laboratory, Soltrace, <https://www.nrel.gov/csp/soltrace.html>
- [12] Petrone, G., *et al.*, Online Identification of PV Source Parameters by Using a Genetic Algorithm, *MDPI Applied Science*, 8 (2018), 1, pp. 1-16
- [13] Perini, S., *et al.*, Theoretical and Experimental Analysis of an Innovative Dual-Axis Tracking Linear Fresnel Lenses Concentrated Solar Thermal Collector, *Solar Energy*, 153 (2017), Sept., pp. 679-690
- [14] Karlsson, B., *et al.*, MaReCo for Large Systems, *Proceedings*, Eurosun 2000 Conference, Copenhagen, 2000
- [15] Gomes, J. L., *et al.*, Minimizing the Impact of Shading at Oblique Solar Angles in a Fully Enclosed Asymmetric Concentrating PVT Collector, *Energy Procedia*, 57 (2014), Nov., pp. 2176-2185
- [16] Torres, J. P. N., *et al.*, The Effect of Shading on PV Solar Panels, *Energy Systems*, 9 (2016), 1, pp. 195-208
- [17] Alves, P., *et al.*, Energy Efficiency of a PV/T Collector for Domestic Water Heating Installed in Sweden or in Portugal, The Impact of Heat Pipe Cross-Section Geometry and Water Flowing Speed, *Proceedings*, 12th Conference on Sustainable Development of Energy, Water and Environment Systems (SDEWES2017), Dubrovnik, Croatia, 2017
- [18] ***, Institute for Energy and Transport, PV Potential Estimation Utility, PV Geographical Information System (PVGIS), 2012, <http://re.jrc.ec.europa.eu/pvgis/apps4/pvest.php?lang=en&map=europe>
- [19] ***, Eclipticsimulator, <http://www.ces.fau.edu/nasa/files/eclipticsimulator.html>
- [20] Gertiga, C., *et al.*, SoFiA – A Novel Simulation Tool for Central Receiver Systems, *Energy Procedia*, 49 (2014), June, pp. 1361-1370
- [21] Adsten, M., Solar Thermal Collectors at High Latitudes, Design and Performance of Non-tracking Concentrators, M. Sc. thesis, Uppsala University, Uppsala, Sweden, 2002